

Implications of a Cosmogenic Origin of KM3-230213A for Ultra-High-Energy Protons

ABDULRAHMAN ALHEBSI ¹, ARJEN VAN VLIET ¹, DOMENIK EHLERT ², AND SATYENDRA THOUDAM ¹

¹*Khalifa University of Science and Technology, Department of Physics, PO Box 127788, Abu Dhabi, UAE*

²*Norwegian University of Science and Technology (NTNU), 7491 Trondheim, Norway*

ABSTRACT

A significant neutrino event with an estimated energy between 72 PeV and 2.6 EeV was recently observed by the KM3NeT experiment (KM3-230213A). When interpreted as cosmogenic in origin, this event can provide constraints on several phenomenological parameters of UHE proton sources. In this study, we present the best fit to the spectrum and composition of UHECRs that is consistent with multi-messenger constraints, including the detection of a single neutrino event by the KM3NeT detector at the energy range of KM3-230213A. From the best fit, we obtain the 68% CL constraints on the parameters of a two-population model of UHECRs, comprising a mixed-composition population and a subdominant UHE proton population. Our results indicate that the detection of a single neutrino event at the energy range of KM3-230213A solely with the KM3NeT exposure requires strongly evolving UHE proton sources, consistent with high-luminosity active galactic nuclei. On the other hand, including the null observations from the Pierre Auger and IceCube observatories disfavors such strong evolution. In both cases, the observed proton fraction of UHECRs is primarily constrained by the composition data to be $\sim 20\%$ at 20 EeV.

Keywords: High-energy astrophysics (739) — Ultra-high-energy cosmic radiation (1733) — Neutrino astronomy (1100) — Cosmic ray sources (328)

1. INTRODUCTION

Ultra-high-energy (UHE) cosmic rays (CRs), with energies $\gtrsim 10^{18}$ eV, are deflected by Galactic and extragalactic magnetic fields, making it challenging to trace them back to their sources. Compounding this challenge are their limited statistics due to their incredibly low flux at the highest energies and their unclear composition due to uncertainties in interpreting measurements of the depth of air shower maximum, X_{\max} . These challenges motivate combining UHECR data with multi-messenger signals to understand the sources of UHECRs.

UHECRs can be studied by examining the cosmogenic neutrino and photon signals they generate through interactions with low-energy photons of the cosmic microwave background (CMB) and extragalactic background light (EBL) during intergalactic propagation. In particular, the observed flux of cosmogenic neutrinos at ~ 1 EeV is largely determined by two properties of UHECRs: (1) the proton fraction of cosmic rays observed at ~ 20 EeV and (2) the cosmological evolution of the sources of these UHE protons. This follows from the

fact that, at energies $\gtrsim 20$ EeV, protons primarily lose energy through photo-pion production, with the decay of the resulting charged pions yielding neutrinos that contribute significantly to the cosmogenic neutrino flux. Furthermore, the cosmological evolution of the emissivity of UHE proton sources determines the number of interactions that occur at high redshift. If the emissivity of proton sources evolves strongly with redshift, more interactions occur at earlier cosmic times, which directly increases the cosmogenic neutrino flux observed on Earth. Hence, an exciting prospect is to combine the observed cosmogenic neutrino flux with UHECR data to place constraints on the observed fraction of UHE protons and the cosmological evolution of their sources. This possibility was noted by H. Takami et al. (2009), M. Ahlers et al. (2009) and N. Globus et al. (2017), and later investigated in detail by A. van Vliet et al. (2019), M. S. Muzio et al. (2023), and D. Ehlert et al. (2024).

The cosmological evolution of UHECR sources remains largely undetermined since the energy-loss length of UHECRs is less than a few Gpc, implying that the observed UHECR flux is dominated by sources within a redshift of $z \sim 1$ (see e.g. T. Stanev et al. 2000). Nevertheless, the observed fluxes of secondary CRs, gamma

rays, and cosmogenic neutrinos set an upper limit on the number of interactions that UHECRs undergo in intergalactic space, and thus on how strongly the UHECR source emissivity can increase with redshift. For a mixed mass composition of UHECRs, for example, a source emissivity evolving with redshift as $\propto (1+z)^5$ or steeper, produces a flux of low-energy secondary CRs that exceeds the observed UHECR spectrum below the ankle ($10^{18.7}$ eV) (R. A. Batista et al. 2019; A. A. Halim et al. 2023). Comparable constraints have also been obtained from diffuse gamma-ray and neutrino upper limits for different composition scenarios of UHECRs, such as mixed-composition scenarios (N. Globus et al. 2017; A. A. Halim et al. 2023), scenarios with a subdominant proton-producing population (M. S. Muzio et al. 2023; D. Ehlert et al. 2024), and the proton dip scenario (J. Heinze et al. 2016; V. Berezhinsky et al. 2016). Because the cosmological evolution varies widely between known source classes, characterizing it for UHECR sources constrains the pool of candidate sources.

The proton fraction of observed UHECRs also remains uncertain, though to a lesser extent than the cosmological evolution of their sources. Information on the mass composition of UHECRs is primarily inferred from extensive air-shower measurements, in particular the distribution of the depth of shower maximum, X_{\max} , in each energy bin. Because interpreting this observable relies on hadronic interaction models, composition inferences carry systematic uncertainties associated with the choice of model (A. Abdul Halim et al. 2024a). The Pierre Auger collaboration has interpreted their observed X_{\max} distributions using different hadronic interaction models (A. Aab et al. 2014; E. Mayotte et al. 2024) and found that all models agree on a very light composition at ~ 3 EeV, which becomes heavier with increasing energy. Although the absolute proton fraction differs between models, they predict a similar trend in the proton fraction with energy, which is characterized by a decrease from $\sim 40 - 60\%$ at ~ 3 EeV to $\sim 0 - 20\%$ at energies $\gtrsim 10$ EeV, within systematic uncertainties. Complementary to air-shower measurements, knowledge of the UHECR composition can be inferred from multi-messenger signals. For a fixed source evolution, cosmogenic neutrino measurements set an upper limit on the number of photo-pion interactions that UHE protons undergo in intergalactic space, and thus on the fraction of protons in the observed UHECR flux. Upper limits on the proton fraction at $10^{19.55}$ eV were obtained for a range of evolution strengths of the source emissivity using upper limits on the UHE ($\gtrsim 10^{16}$ eV) diffuse neutrino flux set by the Pierre Auger (A. Aab et al. 2019) and IceCube (R. Abbasi et al. 2025) observatories.

In this work, we aim to obtain new constraints on the observed fraction of UHE protons and the cosmological evolution of their sources in light of the UHE neutrino event, KM3-230213A (S. Aiello et al. 2025), under the assumption that the event originated from a steady diffuse flux of cosmogenic neutrinos. For this purpose, we use a two-population model of UHECRs adapted from D. Ehlert et al. (2024), comprising a mixed-composition population and a subdominant UHE proton population. Using this model, we perform a joint fit of the spectrum (P. Abreu et al. 2021) and composition observables (A. Abdul Halim et al. 2023) of UHECRs reported by the Pierre Auger Observatory (Auger) while satisfying the detection of a single neutrino event by the Cubic Kilometer Neutrino Telescope (KM3NeT) at the energy range of KM3-230213A, neutrino constraints from IceCube and Auger, and gamma-ray constraints from Auger and the Large Area Telescope on board the *Fermi* gamma-ray space telescope (*Fermi*-LAT). From the best-fit solution, we obtain the 68% CL constraints on the model parameters.

This paper is structured as follows. In Section 2, we describe the model. In Section 3, we present the multi-messenger datasets used in this analysis and discuss the UHE neutrino event, KM3-230213A. In Section 4, we present the method of this analysis and the fit procedure. In Section 5, we present the main results and provide the best-fit parameters. In Section 6, we discuss the viability of the assumptions adopted in this work, and discuss recent studies closely related to our analysis. Lastly, in Section 7, we present the major conclusion of this work.

2. MODEL

2.1. Cosmic-ray Injection Spectra

Our model comprises two independent populations of UHECRs whose sources are distributed isotropically in space. The first population is mixed in composition with five nuclear species: ^1H , ^4He , ^{14}N , ^{28}Si , and ^{56}Fe . The second population is composed purely of protons. For each population, the CR spectrum observed at Earth is dependent on the spectrum of CRs injected into space, which we parameterize as:

$$J_{\text{inj}}(E) = J_0 \sum_A f_A \left(\frac{E}{E_0}\right)^{-\gamma} \exp\left(-\frac{E}{Z_A R_{\max}}\right) \quad (1)$$

Here, γ and R_{\max} are the spectral index and the maximum rigidity of the injected spectrum, respectively, J_0 is a free normalization parameter, E_0 is an arbitrary normalization energy. A represents the nuclear species, Z_A denotes its atomic number, and f_A denotes its compositional fraction at a fixed energy with respect to the total injected spectrum. For the pure-proton popula-

tion $\sum_A f_A = f_p = 1$. It is important to note that the parameters for the two populations are independent.

The two-population model we use is adapted from the model presented in [D. Ehlert et al. \(2024\)](#). Similar to previous studies ([M. S. Muzio et al. 2019, 2023](#)), this work showed that including a subdominant proton component at the highest energies improves fits to the UHECR data. This scenario is consistent with interpretations of the X_{\max} distributions using different hadronic interaction models ([A. Aab et al. 2014](#); [E. Mayotte et al. 2024](#)), all of which predict a subtle increase in the proton fraction around ~ 20 EeV, indicating a possible recovery in the flux of UHE protons. In fact, the data allow for a proton fraction as high as 20% at this energy. These results motivate adopting a model that allows the proton fraction to vary independently of the mixed-composition population. Furthermore, the presence of a subdominant proton population allows the model to reproduce a wide range of cosmogenic neutrino fluxes in light of new observations, while remaining consistent with the UHECR data. On the other hand, typical single-population models exhibit an increasingly heavy composition towards higher energies as a consequence of the Peter’s cycle assumption, where a common maximum rigidity is assumed for all nuclei ([B. Peters 1961](#)), resulting in a relatively low cosmogenic neutrino signal (e.g., [R. A. Batista et al. 2019](#); [J. Heinze et al. 2019](#)).

Compared to the study presented in [D. Ehlert et al. \(2024\)](#), which focused primarily on energies above the ankle, we extend the analysis to lower energies by incorporating a Galactic CR component into the UHECR flux. We adopt the Galactic CR flux from [S. Thoudam et al. \(2016\)](#), in particular, the CR component resulting from supernova explosions in the environment of Wolf-Rayet stars, which dominates at energies between the second knee (10^{17} eV) and the ankle. In our analysis, we consider the normalization of the Galactic component as a free parameter, while keeping the spectral index, the energy cutoff, and the composition fixed at the values reported in [S. Thoudam et al. \(2016\)](#).

2.2. Cosmological Evolution of Sources

The UHECR spectrum observed at Earth also depends on the cosmological evolution of UHECR sources, which we parameterize in our model as:

$$S(z) = \begin{cases} (1+z)^m & \text{for } m \leq 0 \\ (1+z)^m & \text{for } m > 0 \text{ and } z < z_0 \\ (1+z_0)^m & \text{for } m > 0 \text{ and } z_0 < z \leq z_{\max} \\ 0 & \text{for } z > z_{\max}. \end{cases} \quad (2)$$

This function describes how the source emissivity changes with redshift, where m determines the strength and direction (positive or negative) of the evolution. This parameterization, proposed in [A. van Vliet et al. \(2019\)](#), was chosen because typical source candidates show a growth in emissivity up to a redshift $1 \lesssim z \lesssim 1.7$, reach a plateau or increase very slowly up to a redshift $2.7 \lesssim z \lesssim 4$, and then decline beyond that. This behavior is observed in gamma-ray bursts (GRBs) ([D. Wanderman & T. Piran 2010](#)), the star-formation rate (SFR) ([A. M. Hopkins & J. F. Beacom 2006](#)), and AGNs of different luminosity classes ([G. Hasinger et al. 2005](#); [Y. Ueda et al. 2014](#)). In Equation 2, z_0 denotes the redshift beyond which the source emissivity remains constant, and z_{\max} denotes the redshift to which the source population extends. In this analysis, we fix z_0 and z_{\max} to 1.5 and 4, respectively. Since sources differ in the strength of their cosmological evolution, the source-evolution parameter, m , allows us to describe a wide range of sources. For example, the evolution of tidal disruption events is negative and close to $m \sim -3$ ([C. Kochanek 2016](#)), whereas high-luminosity AGNs, such as flat-spectrum radio quasars (FSRQs) and high-luminosity BL Lacertae objects (BL Lacs), have strongly positive evolutions of $m \sim 5 - 7$ ([M. Ajello et al. 2012, 2013](#)).

3. MULTI-MESSENGER DATASETS

The multi-messenger datasets and upper limits used in this study are the following: (1) IceCube’s high-energy event samples, namely High-Energy Starting Events (HESE) ([R. Abbasi et al. 2021](#)), Northern-Sky Tracks (NST) ([R. Abbasi et al. 2022](#)), and the Glashow resonance event ([M. G. Aartsen et al. 2021a](#)); (2) IceCube’s Extremely-High-Energy (IC-EHE) sample (null observations in 12.6 years of livetime, [R. Abbasi et al. 2025](#)); (3) Auger’s null observations of UHE neutrinos (livetime of 18 years, [C. Petrucci et al. 2024](#)); (4) 95% CL upper limits on the diffuse flux of UHE ($\gtrsim 10^{18}$ EeV) gamma rays set by Auger ([P. Abreu et al. 2023](#); [A. Abdul Halim et al. 2024b](#)); (5) the isotropic diffuse gamma-ray background (IGRB) measured by the *Fermi*-LAT ([M. Ackermann et al. 2015](#)); and (6) KM3-230213A ([S. Aiello et al. 2025](#)).

Until recently, no neutrino candidates with energies above $\sim 10^{16}$ eV were detected. This changed on February 13, 2023, when the KM3NeT Astroparticle Research with Cosmics in the Abyss (ARCA) neutrino telescope, currently under construction in the Mediterranean Sea, detected the highest-energy neutrino candidate—KM3-230213A ([S. Aiello et al. 2025](#)). This nearly horizontal-going neutrino event was reconstructed with an energy of approximately 0.220 EeV, with a 90% CL interval of

0.072–2.6 EeV. Given the event’s energy and direction, along with the steep decline of the atmospheric neutrino spectrum at PeV energies (S. Ostapchenko et al. 2023), an astrophysical origin of the event is strongly favored.

While the exact origin of KM3-230213A remains unidentified, different origin scenarios have been investigated, which include a population of steady neutrino emitters, such as blazars (O. Adriani et al. 2025a), a single flaring blazar (P. Baldini et al. 2025; G. F. de Clairfontaine et al. 2025), other transient phenomena (F. Nozzoli 2025; A. Neronov et al. 2025), cosmogenic production (O. Adriani et al. 2025b; M. S. Muzio et al. 2025; M. Y. Kuznetsov et al. 2025a; A. Cermenati et al. 2025), a galactic origin (O. Adriani et al. 2025c), or heavy dark matter decay (D. Borah et al. 2025; K. Kohri et al. 2025). The hypothesis that KM3-230213A originates from a steady diffuse astrophysical component not yet identified by existing experiments cannot be ruled out, given that the probability of observing one event by KM3NeT and none by the Pierre Auger and IceCube observatories is about 0.4% when considering the combined exposure of all three experiments to UHE neutrinos (R. Abbasi et al. 2025). Moreover, directional associations of KM3-230213A to blazar candidates do not rule out a cosmogenic origin scenario. This is because high-rigidity CRs escaping their source environments close to our line of sight can interact with background photons before getting significantly deflected by intergalactic magnetic fields, creating ‘line-of-sight’ cosmogenic neutrinos (S. Das et al. 2025).

Because we are concerned with the cosmogenic component of astrophysical neutrinos, the multi-messenger datasets that we aim to explain with our model are KM3-230213A and neutrino upper limits reported by IceCube and Auger above ~ 5 PeV, which we shall refer to as the UHE neutrino datasets. The remaining datasets, which include the neutrino flux below ~ 5 PeV from IceCube’s high-energy event samples, the IGRB flux, and Auger’s upper limits on the UHE gamma-ray flux, serve only as limits not to be exceeded (see Section 4). In particular, we constrain the model-predicted GeV–TeV gamma-ray flux to contribute no more than 40% of the IGRB, since unresolved gamma-ray sources are predicted to account for at least the remaining 60% (M. Lisanti et al. 2016; M. Ackermann et al. 2016).

4. METHOD

We use the simulation framework CRPROPA 3.2 (R. Alves Batista et al. 2022) to produce Monte Carlo events of propagated UHECRs and their secondary cosmogenic neutrinos and gamma rays. We use the EBL model from (R. C. Gilmore et al. 2012) and photodisintegration cross

sections obtained from the TALYS model (A. J. Koning et al. 2007). The composition observables we fit are the mean $\langle X_{\max} \rangle$ and the standard deviation $\sigma(X_{\max})$ of the X_{\max} distribution in each energy bin (A. Abdul Halim et al. 2023). To compare our model with these observables, we convert the average atomic mass in each energy bin into these quantities using the parameterization of P. Abreu et al. (2013) for the EPOS-LHC³ hadronic interaction model.

We fit the data by minimizing the deviance, $D = -2 \ln(L/L_{\text{sat}})$, which is equivalent to maximizing the model’s likelihood, L , where L_{sat} is the likelihood of a saturated model that perfectly describes the data. For the UHECR spectrum and composition, we assume Gaussian likelihood distributions:

$$D_{\text{CR}} = \sum_F \sum_i \left[\frac{F_{\text{Auger}}(E_i) - F_{\text{model}}(E_i; \mathbf{P})}{\sigma_i} \right]^2, \quad (3)$$

computed for a set of parameter values, \mathbf{P} , for three Auger observables $F \in \{J_{\text{CR}}, \langle X_{\max} \rangle, \sigma(X_{\max})\}$ at each i -th energy bin in $E \geq 10^{17.85}$ eV. For the UHE neutrino datasets, we assume Poissonian likelihood distributions:

$$D_{\text{UHE } \nu} = 2 \sum_d \sum_i \mu_d^i - n_d^i + n_d^i \ln(n_d^i/\mu_d^i) \quad (4)$$

where μ_d^i and n_d^i are the expected and observed number of events, respectively, at the i -th energy bin of dataset $d \in \{\text{Auger, KM3NeT, IC-EHE, HESE}(> 5 \text{ PeV}), \text{NST}(> 5 \text{ PeV})\}$. For energy bins with zero observed events, i.e., outside the 90% CL interval of KM3-230213A, the deviance simplifies to $2\mu_d$, which is given by:

$$\mu_d = \frac{1}{3} \int_{E_{\min,d}}^{E_{\max,d}} \mathcal{E}_d^{\text{all-flavor}}(E) \times \Phi_{\nu+\bar{\nu}}^{\text{all-flavor}}(E) dE \quad (5)$$

where $\Phi_{\nu+\bar{\nu}}^{\text{all-flavor}}$ is the model-predicted all-flavor neutrino flux and $\mathcal{E}_d^{\text{all-flavor}}$ is the sky-averaged, all-flavor detector exposure corresponding to dataset d . Both quantities are averaged between neutrinos and anti-neutrinos. The integration is carried over the energy range of the dataset $[E_{\max,d}, E_{\min,d}]$, and the result is multiplied by 1/3 to return the expected number of events from a single neutrino flavor. The detector exposures of Auger, IceCube, and KM3NeT/ARCA used to calculate Equation 4 were obtained from C. Petrucci et al. (2024), R. Abbasi et al. (2025), and O. Adriani et al. (2025d), respectively.

³ Parameter values were obtained through private communication with S. Petrerá.

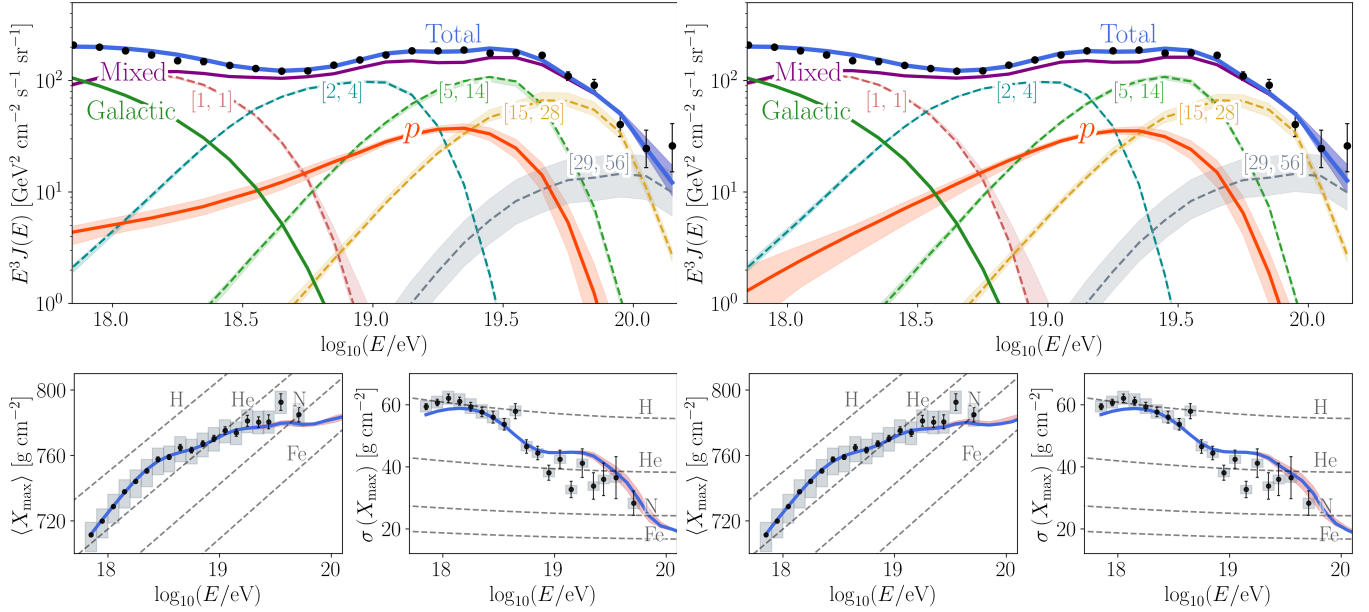


Figure 1. The CR spectrum (top) and composition observables (bottom) of the KM3NeT-only (left) and joint (right) fits shown alongside data by Auger (P. Abreu et al. 2021; A. Abdul Halim et al. 2023). The contribution of different mass groups is shown with $[A_{\text{min}}, A_{\text{max}}]$, and colored bands indicate the 68% CL range. The Galactic component is added to our model from S. Thoudam et al. (2016), albeit with a free normalization. In the lower panels, the EPOS-LHC hadronic interaction model is used to interpret different nuclei (grey dashed lines) and the model-predicted composition (solid blue line) into $\langle X_{\text{max}} \rangle$ and $\sigma(X_{\text{max}})$.

For the neutrino flux below ~ 5 PeV from IceCube’s high-energy event samples, the IGRB flux, and Auger’s upper limits on the UHE gamma-ray flux, we use a one-sided Gaussian likelihood deviance that contributes only when the predicted flux exceeds the observed flux, thereby acting as a penalty term which we denote by D_{penalty} . The total deviance for the minimization then becomes $D = D_{\text{CR}} + D_{\text{UHE } \nu} + D_{\text{penalty}}$.

5. RESULTS

The best-fit solution is determined for two scenarios. In the first scenario, neutrino upper limits from Auger and IceCube are disregarded, and Equation 4 is evaluated using only the KM3NeT dataset. We refer to this as the KM3NeT-only fit. In the second scenario, Equation 4 is evaluated for all three detectors, and we refer to this as the joint fit.

Figure 1 shows the spectrum (upper panels) and composition observables (lower panels) of UHECRs arriving at Earth as reported by Auger (P. Abreu et al. 2021; A. Abdul Halim et al. 2023), together with model predictions of the KM3NeT-only (left panels) and joint (right panels) fits. We have divided the mixed-composition population in our model into five components corresponding to the five injected species of ^1H , ^4He , ^{14}N , ^{28}Si , and ^{56}Fe . The other two components shown are the Galactic CRs and the subdominant UHE proton population. Both fits predict a relatively hard spectral index of

the injected spectra for both the mixed-composition and the pure-proton populations. In both populations, the flux suppression is dominated by the maximum rigidity cutoff at the sources.

Both fits exhibit a similar evolution of the proton fraction in the observed spectrum, peaking to $\sim 65\%$ at ~ 2 EeV, predominantly due to secondary protons produced by photodisintegration of heavier nuclei in the mixed-composition population. Above that energy, the contribution from the subdominant proton population increases steadily until ~ 20 EeV, where the proton fraction reaches a second peak of $\sim 20\%$. Beyond this point, it declines until becoming negligible at energies $\gtrsim 100$ EeV. For each fit, we report the observed proton fraction only at 20 EeV, which we denote by $f_p^{\text{obs}}(20 \text{ EeV})$. The elemental fractions of the mixed-composition population before propagation are reported at a fixed rigidity, f_A^R , such that the ratio of the flux of element A to the total flux is reported at the same rigidity for all elements⁴.

Figure 2 shows the corresponding cosmogenic gamma-ray and neutrino spectra predicted by the KM3NeT-only (left panel) and joint (right panel) fits, plotted alongside the IGRB data by *Fermi*-LAT (M. Acker-

⁴ A transformation between f_A^R and the fraction at a fixed energy defined in Equation 1 can be achieved via $f_A^R = f_A \cdot Z(A)^{1-\gamma}$.

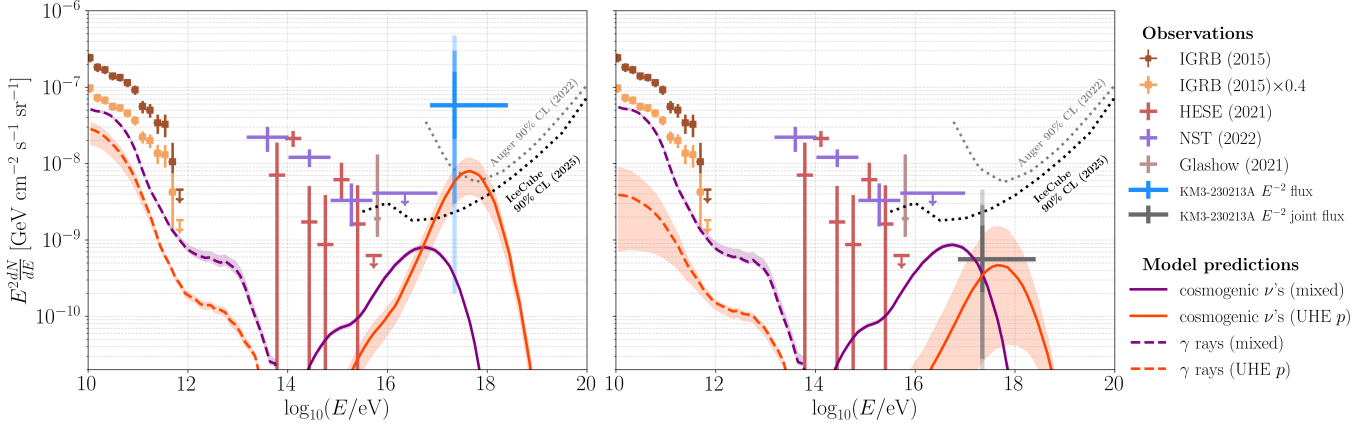


Figure 2. Cosmogenic neutrinos (solid lines) and diffuse electromagnetic-cascade gamma rays (dashed lines) of the KM3NeT-only (left) and joint (right) fits. All neutrino fluxes are per-flavor, assuming flavor equipartition post-propagation. Contributions from the mixed and pure-proton populations are shown in purple and orange, respectively, with bands indicating the 68% CL range. We show the IGRB measured by *Fermi*-LAT, IceCube’s high-energy event samples (High-Energy Starting Events (HESE), Northern-Sky Tracks (NST), and the Glashow resonance event), as well as the 90% CL neutrino upper limits reported by IceCube and Auger. We also show the E^{-2} flux associated with KM3-230213A (see main text), for which the horizontal error bar represents the 90% CL interval on the estimated neutrino energy, and the vertical error bars represent the 68%, 95%, and 97.5% Feldman-Cousins confidence intervals (G. J. Feldman & R. D. Cousins 1998).

mann et al. 2015), IceCube’s high-energy event samples (R. Abbasi et al. 2021; M. G. Aartsen et al. 2021a; R. Abbasi et al. 2022), and the UHE neutrino upper limits by Auger (J. Alvarez-Muñiz et al. 2025) and IceCube (R. Abbasi et al. 2025). Alongside the KM3NeT-only fit, we plot the single-flavor E^{-2} flux for KM3-230213A reported in S. Aiello et al. (2025), which is based solely on the KM3NeT/ARCA exposure. In the joint-fit panel, we plot the corresponding E^{-2} flux derived from the combined exposures of Auger, IceCube, and KM3NeT/ARCA obtained from C. Petrucci et al. (2024), R. Abbasi et al. (2025), and O. Adriani et al. (2025d), respectively, which we calculate⁵ to be $E^2\Phi_{\nu+\bar{\nu}}^{1f} = 5.6_{-3.5}^{+9.8} \times 10^{-10} \text{ GeV}^{-1} \text{ cm}^{-2} \text{ s}^{-1} \text{ sr}^{-1}$ with the 68% Feldman-Cousins confidence interval (G. J. Feldman & R. D. Cousins 1998).

Figure 3 shows the range of the predicted integral flux of UHE gamma rays observed on Earth from the KM3NeT-only and joint fits at the 68% CL, along with upper limits from Auger (P. Abreu et al. 2023; A. Abdul Halim et al. 2024b) and the Telescope Array (R. U. Abbasi et al. 2019). No penalty was applied to the total deviance in either fit for this observable since all upper limits were far from being exceeded.

⁵ The method for this calculation is detailed in (O. Adriani et al. 2025d), where an estimate of $E^2\Phi_{\nu+\bar{\nu}}^{1f} = 7.5_{-4.7}^{+13.1} \times 10^{-10} \text{ GeV}^{-1} \text{ cm}^{-2} \text{ s}^{-1} \text{ sr}^{-1}$ was obtained using the 9-year IceCube exposure (M. G. Aartsen et al. 2018), as opposed to the 12.6-year exposure used for our estimate.

We obtain the following 68% CL constraints on the source-evolution parameter of the pure-proton population m^p and the observed proton fraction $f_p^{\text{obs}}(20 \text{ EeV})$ from the KM3NeT-only fit:

$$5.2 \leq m^p \leq 6.6 \quad (6)$$

$$18.9\% \leq f_p^{\text{obs}}(20 \text{ EeV}) \leq 21.9\%$$

and from the joint fit:

$$-1.2 \leq m^p \leq 4.1 \quad (7)$$

$$18.1\% \leq f_p^{\text{obs}}(20 \text{ EeV}) \leq 20.8\%$$

The remaining best-fit parameters are reported in Table 1.

In both fits, the observed proton fraction is tightly constrained by $\sigma(X_{\text{max}})$ at the upper bound and by $\langle X_{\text{max}} \rangle$ at the lower bound. Hence, our fits predict an observed proton fraction of $f_p^{\text{obs}}(20 \text{ EeV}) \sim 20\%$ under EPOS-LHC, which constrains the source-evolution parameter m^p to the ranges above, under the two scenarios for the observed cosmogenic neutrino flux. In the scenario where only the KM3NeT dataset is considered, the detection of KM3-230213A favors a strong positive source evolution for the sources of UHE protons. In this scenario, m^p is constrained at the upper bound by the IGRB flux, and at the lower bound by the non-zero event count in the KM3NeT dataset. In the scenario where the UHE neutrino datasets of Auger, IceCube, and KM3NeT are considered, m^p is constrained to a wider range of lower values, including flat ($m^p = 0$) and

slightly negative source evolutions. In this scenario, m^p is constrained at the upper bound by the zero event count in the Auger and IceCube datasets at the energy range of KM3-230213A, and at the lower bound by the non-zero event count in the KM3NeT dataset.

Several high-luminosity ($\gtrsim 10^{46}$ erg s $^{-1}$) classes of AGNs show a strong positive evolution of emissivity with redshift. AGNs tend to have a luminosity-dependent density evolution (Y. Ueda et al. 2003; G. Hasinger et al. 2005), whereby the growth of the source density with redshift and the redshift at which it peaks (corresponding roughly to m and z_0 , respectively, in Equation 2) may depend on the luminosity class of the AGN. AGN classes with a source density evolution consistent with that of the pure-proton population in the KM3NeT-only fit (Inequality 6) include: FSRQs with luminosity 10^{48} erg s $^{-1}$, whose density grows as $(1+z)^{7.4}$ up to $z \sim 1.5$ and then declines as $(1+z)^{-6.5}$ (M. Ajello et al. 2012); BL Lacs with luminosity 10^{47} erg s $^{-1}$, whose density grows as $(1+z)^{7.2}$ up to $z \sim 1.3$ and then declines as $(1+z)^{-7.4}$ (M. Ajello et al. 2013); and high-luminosity ($10^{46} - 10^{47}$ erg s $^{-1}$) non-jetted AGNs, whose density grows as $(1+z)^{5.9}$ up to $z \sim 1.9$ and then declines as $(1+z)^{-1.5}$ (Y. Ueda et al. 2014). In addition to satisfying Inequality 6, high-luminosity BL Lacs and FSRQs can produce a proton-dominated emission of UHECRs, if CRs are accelerated efficiently (X. Rodrigues et al. 2021), making them plausible candidates for a subdominant UHE proton population. Another candidate source of UHE protons is high-luminosity ($\gtrsim 10^{50}$ erg s $^{-1}$) GRBs, whose jets are expected to be dominated by protons and neutrons in the classical fireball scenario (S. Horiuchi et al. 2012). The cosmological evolution of GRBs has been linked to the SFR ($m \sim 3$ in Equation 2, H. Yüksel et al. 2008), but other studies predict a weaker evolution of $m \sim 2$ (D. Wanderman & T. Piran 2010; A. Lien et al. 2014), or a negative evolution of $m \sim -1$ (V. Petrosian et al. 2015), all of which are consistent with the source evolution of the pure-proton population in the joint-fit (Inequality 7). Other source classes consistent with Inequality 7 include: star-forming galaxies ($m \sim 3$, A. M. Hopkins 2004; A. M. Hopkins & J. F. Beacom 2006; P. Madau & M. Dickinson 2014), low-radio-power AGNs ($m \sim 1$, V. Smolčić et al. 2009), low-luminosity ($10^{43} - 10^{45}$ erg s $^{-1}$) non-jetted AGNs ($m \sim 0 - 3$, Y. Ueda et al. 2014), and intermediate-luminosity (10^{46} erg s $^{-1}$) BL Lacs and FSRQs ($m \sim 0$, M. Ajello et al. 2012, 2013).

Neutrino and gamma-ray observations also constrain the spectral features of the pure-proton population. Harder proton spectra are favored since they produce fewer low-energy protons and hence fewer low-energy

Table 1. The 68% CL intervals around the best-fit parameters. The number of degrees of freedom are $N_{\text{dof, CR}} = 49$ and $N_{\text{dof, UHE } \nu} = 2$ from the two Poissonian distributions inside and outside the energy range of KM3-230213A. Confidence intervals that touch the boundaries of the parameter space are indicated by an asterisk.

Best fit	KM3NeT-only	Joint
Mixed-composition population		
γ	$-2.77_{-0.11}^{+0.11}$	$-2.78_{-0.13}^{+0.13}$
R_{max} [EV]	$1.23_{-0.03}^{+0.03}$	$1.24_{-0.04}^{+0.03}$
m	$3.9_{-0.1}^{+0.1}$	$4.0_{-0.1}^{+0.1}$
f_{H}^R [%]	$0.2_{-0.2}^{+6.8}$	$0.3_{-0.3}^{+9.5}$
f_{He}^R [%]	$50.5_{-5.2}^{+5.1}$	$47.0_{-5.1}^{+2.6}$
f_{N}^R [%]	$41.9_{-5.5}^{+5.5}$	$45.4_{-6.5}^{+5.5}$
f_{Si}^R [%]	$7.0_{-0.9}^{+0.7}$	$7.0_{-1.5}^{+0.7}$
f_{Fe}^R [%]	$0.39_{-0.15}^{+0.26}$	$0.43_{-0.16}^{+0.25}$
Pure-proton population		
γ^p	$-1.66_{-1.34*}^{+1.18}$	$-0.05_{-0.88}^{+0.66}$
R_{max}^p [EV]	$7.18_{-1.96}^{+2.82}$	$10.01_{-2.30}^{+2.95}$
m^p	$6.1_{-0.9}^{+0.5}$	$2.5_{-3.7}^{+1.6}$
$f_p(20 \text{ EeV})$ [%]	$20.3_{-1.4}^{+1.6}$	$19.4_{-1.3}^{+1.4}$
D/N_{dof}	155.4/51	165.2/55

interactions. Here, we refer specifically to electron-positron pair production interactions with the CMB and photo-pion production interactions with the EBL. The former is a significant contributor to the diffuse GeV–TeV gamma-ray flux, which is constrained by the *Fermi*-LAT data, and the latter contributes to the neutrino flux at $10^{15} - 10^{17}$ eV, which is constrained by the IceCube high-energy event samples. The maximum rigidity of UHE protons, R_{max}^p , is constrained to values below the GZK limit of ~ 50 EeV (K. Greisen 1966; G. T. Zatsepin & V. A. Kuz'min 1966) in both fits by the measurements of $\sigma(X_{\text{max}})$, which disfavors a pure-proton composition at the highest energy bins, and the null observations of neutrinos beyond the energy range of KM3-230213A, which are expected to be abundant if UHE protons exceed the GZK limit (O. E. Kalashev et al. 2002). These findings on the spectral index and maximum rigidity of a subdominant UHE proton component are in agreement with those of D. Ehlert et al. (2024), who find that a hard proton spectrum with a sub-GZK maximum rigidity is most compatible with the UHECR and multi-messenger data.

6. DISCUSSION

The detection of a ~ 0.2 EeV neutrino by the KM3NeT/ARCA detector could be the first observation of a cosmogenic neutrino. If interpreted as cosmogenic,

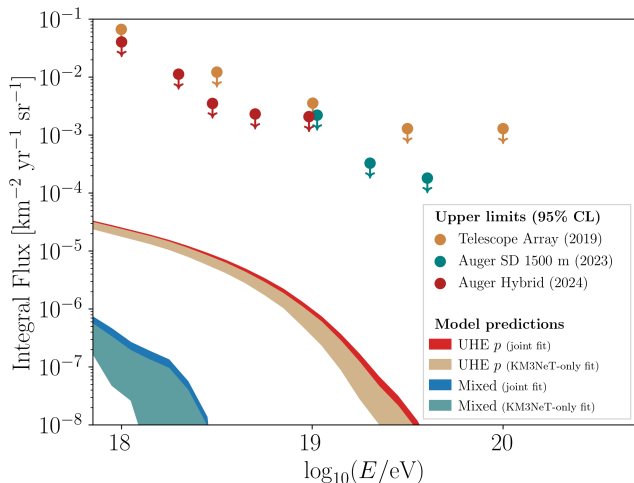


Figure 3. The 68% CL range in the model-predicted integral flux of UHE gamma rays and current 95% CL upper limits posed by Auger (P. Abreu et al. 2023; A. Abdul Halim et al. 2024b) and the Telescope Array (R. U. Abbasi et al. 2019).

the KM3-230213A event could constrain two important properties of UHECRs: the observed fraction of UHE protons and the cosmological evolution of their sources. We have adopted a scenario in which the UHECRs observed on Earth originate from two independent populations extending to $z_{\text{max}} = 4$. The first population is mixed in composition, while the second population is comprised of UHE protons that contribute subdominantly to the CR spectrum. We used KM3-230213A and multi-messenger upper limits to place constraints on the UHE proton population. We found that KM3-230213A and multi-messenger upper limits only constrain the cosmological evolution of the sources of UHE protons, whereas the observed proton fraction is primarily constrained by the UHECR data. Under the hadronic interaction model EPOS-LHC, the X_{max} data constrain the observed proton fraction to $f_p(20 \text{ EeV}) \sim 20\%$, which in turn constrains the strength of the source evolution of UHE protons to $m^p = 6.1_{-0.9}^{+0.5}$ when considering only the KM3NeT UHE neutrino dataset, and to $m^p = 2.5_{-3.7}^{+1.6}$ when the null observations of Auger and IceCube are taken into account.

In this work, we have ignored source-to-source variations in a single population. It has been shown that UHECR sources act as standard candles since the source-to-source variation in the maximum rigidity is surprisingly low (D. Ehlert et al. 2023). We have also assumed an isotropic distribution of sources, even at low redshifts. This assumption was tested in A. A. Halim et al. (2023), where it was shown that modeling the local ($\lesssim 100 \text{ Mpc}$) overdensity of sources had no signifi-

cant effect on the quality of the fit to the spectrum and composition of UHECRs. Furthermore, a local overdensity of sources contributes negligibly to the total flux of cosmogenic secondaries compared to the cumulative contribution from sources at greater distances.

The values for the spectral index and the maximum rigidity of any injected spectrum that best fit the measured UHECR spectrum depend on the shape of the energy cutoff. Functions that model the energy cutoff include a simple exponential, a broken exponential, which is equal to 1 if $E < ZR_{\text{max}}$ and $\exp(1 - E/ZR_{\text{max}})$ if $E \geq ZR_{\text{max}}$, or a hyperbolic secant given by $\text{sech}[(E/ZR_{\text{max}})^\Delta]$, where Δ relates to the steepness and width of the energy cutoff. In A. A. Halim et al. (2023) and T. Bister & G. R. Farrar (2024), the measured UHECR spectrum is fitted using different energy cutoffs. They have shown that simple and broken exponential cutoffs require very hard injected spectra ($\propto E^{-\gamma}$ where $\gamma \sim -2$) to reproduce the observed energy spectrum, as is the case in this work. In contrast, sharper cutoffs, such as a hyperbolic secant with $\Delta = 2$, fit the data with much softer spectra ($\gamma \sim 0.3 - 0.7$), and even softer ($\gamma \sim 1$) for $\Delta = 3$, closer to expectations from known acceleration processes (see also L. Comisso et al. 2024). Despite this, the authors have shown that the fit quality remains superior for simple and broken exponential cutoffs. Various studies have demonstrated that the spectral index is anti-correlated with the source-evolution parameter m (A. M. Taylor et al. 2015; A. Aab et al. 2017; J. Heinze et al. 2019; R. A. Batista et al. 2019). This implies that a softer injection spectrum of UHE protons, resulting from choosing a steeper energy cutoff, could lower the best-fit value of m^p found in this work.

One simplification implemented in this study that could also influence the best-fit value of the spectral index is the omission of intergalactic magnetic fields. It was demonstrated in D. Wittkowski et al. (2017), S. Mollerach & E. Roulet (2020), and J. M. González et al. (2021) that a low source density, where the average separation between UHECR sources is large enough ($\gtrsim 10 \text{ Mpc}$), together with relatively strong intergalactic magnetic fields ($\sim 1 \text{ nG}$), give rise to the so-called magnetic horizon effect (R. Aloisio & V. Berezhinsky 2005). This effect suppresses the low-energy CR flux, thereby hardening the spectrum. By amplifying this effect, the authors were able to fit the UHECR spectrum with much softer injection spectra than when intergalactic magnetic fields are neglected. Nonetheless, the case for strong intergalactic magnetic fields and low source densities that lead to the magnetic horizon effect remains an assumption not required by data.

Several studies have investigated the possibility that KM3-230213A originated from a steady cosmogenic neutrino component. It was demonstrated in [O. Adriani et al. \(2025b\)](#) that a mixed-composition population of UHECRs propagating from a redshift of $z_{\max} = 6$, possibly with an additional subdominant proton component at UHEs, can contribute partially to the diffuse neutrino flux associated with the detection of KM3-230213A. Another implementation of the subdominant proton population scenario is presented in [A. Cerumenati et al. \(2025\)](#), where it is shown that a hard subdominant proton spectrum with a maximum rigidity of 100 EeV can explain KM3-230213A without violating any multi-messenger limits if the source emissivity evolves as $(1+z)^3$ up to $z_{\max} = 5$. Their results partially align with our joint fit; however, whereas we investigate the entire parameter space, their analysis is limited to two scenarios for the proton spectrum, neither of which fully resembles our best-fit proton spectrum, making a direct comparison difficult.

Similar to this work, [M. S. Muzio et al. \(2025\)](#) jointly fits the UHECR and neutrino data but under two scenarios for the true energy of the detected neutrino: 100 PeV and 1 EeV. They conclude that a 100 PeV neutrino can be explained by source neutrinos, whereas a 1 EeV neutrino strongly suggests a cosmogenic origin and hence the presence of an additional subdominant UHE proton population from which the observed neutrino was produced. Unlike this work, however, the authors assume a source evolution following the SFR up to a maximum comoving distance of 4.2 Gpc ($z \sim 1.5$) throughout their study and do not report the quantitative constraints KM3-230213A places on their model parameters.

Another attempt to interpret the UHE neutrino event in light of UHECR observations was made using the Telescope Array (TA) data ([M. Y. Kuznetsov et al. 2025b](#)). The authors refer back to two fits for the UHECR spectrum and composition reported by the TA collaboration ([D. Bergman 2021](#)) and show that these are compatible with the detection of KM3-230213A and the null observations by Auger, IceCube, and the Baikal-GVD experiment, at approximately the 2σ level. The TA fits predict a composition dominated by protons above the ankle. This naturally enhances the production of cosmogenic neutrinos at ~ 1 EeV, resulting in better agreement with the KM3NeT dataset. However, such a composition is not compatible with the X_{\max} data reported by Auger.

7. CONCLUSION

We have used KM3-230213A and multi-messenger upper limits to place constraints on an UHE proton

population that contributes subdominantly to the observed UHECR spectrum above the ankle. We find that the detection of a single neutrino event at the energy range of KM3-230213A solely with the KM3NeT exposure requires that the sources of the currently undiscovered UHE proton population must have a strong positive cosmological evolution, equivalent to the evolution of high-luminosity FSRQs, BL Lacs, and non-jetted AGNs. On the other hand, including the null observations from the Pierre Auger and IceCube observatories disfavors sources with strong positive cosmological evolutions as the origin of the UHE proton population. Instead, sources with a moderately positive, flat, or slightly negative evolution become favorable, such as GRBs, star-forming galaxies, low-radio-power AGNs, low-luminosity non-jetted AGNs, and intermediate-luminosity FSRQs and BL Lacs. In both scenarios, the X_{\max} data constrain the observed proton fraction of UHECRs to be $\sim 20\%$ at 20 EeV.

Observations by future UHECR and neutrino observatories will significantly improve our results. One of the major goals of the Pierre Auger Observatory upgrade, the AugerPrime, is to assess the possible existence of a proton component at the highest energies ([A. Castellina 2019](#)), and hence determine the fraction of protons in observed UHECRs. The presence of a proton component at the highest energies would improve the prospects for UHECR astronomy, since protons are less strongly deflected by magnetic fields than heavier nuclei. At the same time, the ongoing operation and construction of current neutrino telescopes such as KM3NeT/ARCA ([S. Aiello et al. 2024](#)) and Baikal-GVD ([V. Allakhverdyan et al. 2023](#)), and the planned operation of next-generation neutrino telescopes, such as GRAND ([J. Álvarez-Muñiz et al. 2020](#)), RNO-G ([J. A. Aguilar et al. 2021](#)), IceCube-Gen2 ([M. G. Aartsen et al. 2021b](#)), P-ONE ([P. Malecki 2024](#)), NEON ([H. Zhang et al. 2025](#)), TRIDENT ([Z. Ye et al. 2023](#)), and HUNT ([M. Chen et al. 2026](#)), will substantially increase event statistics, allowing for a more precise determination of the cosmogenic neutrino flux.

ACKNOWLEDGMENTS

AA, AvV, and ST acknowledge support from Khalifa University's internal grants, RIG-S-2023-070 and RIG-2024-047. AA acknowledges the use of the KM3NeT's collaboration computing resources to produce the results of this study. AA would like to thank Ralph Engel, Maximilian Meier, and Sergey Troitsky for useful discussions. AA would also like to thank Sergio Petrera for

providing parameter values of the parameterization in P. Abreu et al. (2013) for the EPOS-LHC model.

AUTHOR CONTRIBUTIONS

AA led the analysis and was responsible for writing and submitting the manuscript. AvV developed the idea for

this study. DE assisted with the analysis and idea development. ST provided data and assisted with the idea development. All authors equally contributed to reviewing and editing the manuscript.

REFERENCES

- Aab, A., Abreu, P., Aglietta, M., et al. 2014, *Physical Review D*, 90, 122006, doi: [10.1103/PhysRevD.90.122006](https://doi.org/10.1103/PhysRevD.90.122006)
- Aab, A., Abreu, P., Aglietta, M., et al. 2017, *Journal of Cosmology and Astroparticle Physics*, 2017, 038, doi: [10.1088/1475-7516/2017/04/038](https://doi.org/10.1088/1475-7516/2017/04/038)
- Aab, A., Abreu, P., Aglietta, M., et al. 2019, *Journal of Cosmology and Astroparticle Physics*, 2019, 022, doi: [10.1088/1475-7516/2019/10/022](https://doi.org/10.1088/1475-7516/2019/10/022)
- Aartsen, M. G., Ackermann, M., Adams, J., et al. 2018, *Physical Review D*, 98, 062003, doi: [10.1103/PhysRevD.98.062003](https://doi.org/10.1103/PhysRevD.98.062003)
- Aartsen, M. G., Abbasi, R., Ackermann, M., et al. 2021a, *Nature*, 591, 220, doi: [10.1038/s41586-021-03256-1](https://doi.org/10.1038/s41586-021-03256-1)
- Aartsen, M. G., Abbasi, R., Ackermann, M., et al. 2021b, *Journal of Physics G: Nuclear and Particle Physics*, 48, 060501, doi: [10.1088/1361-6471/abbd48](https://doi.org/10.1088/1361-6471/abbd48)
- Abbasi, R., Ackermann, M., Adams, J., et al. 2021, *Physical Review D*, 104, 022002, doi: [10.1103/PhysRevD.104.022002](https://doi.org/10.1103/PhysRevD.104.022002)
- Abbasi, R., Ackermann, M., Adams, J., et al. 2022, *The Astrophysical Journal*, 928, 50, doi: [10.3847/1538-4357/ac4d29](https://doi.org/10.3847/1538-4357/ac4d29)
- Abbasi, R., Ackermann, M., Adams, J., et al. 2025, *Physical review letters*, 135, 031001, doi: [10.1103/PhysRevLett.135.031001](https://doi.org/10.1103/PhysRevLett.135.031001)
- Abbasi, R. U., Abe, M., Abu-Zayyad, T., et al. 2019, *Astroparticle physics*, 110, 8, doi: [10.1016/j.astropartphys.2019.03.003](https://doi.org/10.1016/j.astropartphys.2019.03.003)
- Abdul Halim, A., Abreu, P., Aglietta, M., et al. 2023, in 38th International Cosmic Ray Conference (ICRC2023)-Cosmic-Ray Physics (Indirect, CRI), 319, doi: [10.22323/1.444.0319](https://doi.org/10.22323/1.444.0319)
- Abdul Halim, A., Abreu, P., Aglietta, M., et al. 2024a, *Physical Review D*, 109, 102001, doi: [10.1103/PhysRevD.109.102001](https://doi.org/10.1103/PhysRevD.109.102001)
- Abdul Halim, A., Abreu, P., Aglietta, M., et al. 2024b, *Physical Review D*, 110, 062005, doi: [10.1103/PhysRevD.110.062005](https://doi.org/10.1103/PhysRevD.110.062005)
- Abreu, P., Aglietta, M., Ahlers, M., et al. 2013, *Journal of Cosmology and Astroparticle Physics*, 2013, doi: [10.1088/1475-7516/2013/02/026](https://doi.org/10.1088/1475-7516/2013/02/026)
- Abreu, P., Aglietta, M., Albury, J. M., et al. 2021, *The European Physical Journal C*, 81, 1, doi: [10.1140/epjc/s10052-021-09700-w](https://doi.org/10.1140/epjc/s10052-021-09700-w)
- Abreu, P., Aglietta, M., Allekotte, I., et al. 2023, *Journal of cosmology and astroparticle physics*, 2023, 021, doi: [10.1088/1475-7516/2023/05/021](https://doi.org/10.1088/1475-7516/2023/05/021)
- Ackermann, M., Ajello, M., Albert, A., et al. 2015, *The Astrophysical Journal*, 799, 86, doi: [10.1088/0004-637X/799/1/86](https://doi.org/10.1088/0004-637X/799/1/86)
- Ackermann, M., Ajello, M., Albert, A., et al. 2016, *Physical Review Letters*, 116, 151105, doi: [10.1103/PhysRevLett.116.151105](https://doi.org/10.1103/PhysRevLett.116.151105)
- Adriani, O., Albert, A., Alhebsi, A., et al. 2025a, arXiv preprint arXiv:2511.13886, doi: [10.48550/arXiv.2511.13886](https://doi.org/10.48550/arXiv.2511.13886)
- Adriani, O., Aiello, S., Albert, A., et al. 2025b, *The Astrophysical Journal Letters*, 984, L41, doi: [10.3847/2041-8213/adcc29](https://doi.org/10.3847/2041-8213/adcc29)
- Adriani, O., Aiello, S., Albert, A., et al. 2025c, arXiv preprint arXiv:2502.08387, doi: [10.48550/arXiv.2502.08387](https://doi.org/10.48550/arXiv.2502.08387)
- Adriani, O., Aiello, S., Albert, A., et al. 2025d, *Physical Review X*, 15, 031016, doi: [10.1103/yypk-zmb8](https://doi.org/10.1103/yypk-zmb8)
- Aguilar, J. A., Allison, P., Beatty, J., et al. 2021, *Journal of Instrumentation*, 16, P03025, doi: [10.1088/1748-0221/16/03/P03025](https://doi.org/10.1088/1748-0221/16/03/P03025)
- Ahlers, M., Anchordoqui, L. A., & Sarkar, S. 2009, *Physical Review D—Particles, Fields, Gravitation, and Cosmology*, 79, 083009, doi: [10.1103/PhysRevD.79.083009](https://doi.org/10.1103/PhysRevD.79.083009)
- Aiello, S., Albert, A., Alshamsi, M., et al. 2024, *The European Physical Journal C*, 84, 885, doi: [10.1140/epjc/s10052-024-13137-2](https://doi.org/10.1140/epjc/s10052-024-13137-2)
- Aiello, S., Albert, A., Alhebsi, A. R., et al. 2025, *Nature*, 638, 376, doi: [10.1038/s41586-024-08543-1](https://doi.org/10.1038/s41586-024-08543-1)
- Ajello, M., Shaw, M., Romani, R., et al. 2012, *The Astrophysical Journal*, 751, 108, doi: [10.1088/0004-637X/751/2/108](https://doi.org/10.1088/0004-637X/751/2/108)
- Ajello, M., Romani, R., Gasparrini, D., et al. 2013, *The Astrophysical Journal*, 780, 73, doi: [10.1088/0004-637X/780/1/73](https://doi.org/10.1088/0004-637X/780/1/73)

- Allakhverdyan, V., Avrorin, A., Avrorin, A., et al. 2023, *Bulletin of the Russian Academy of Sciences: Physics*, 87, 1059, doi: [10.3103/S1062873823702817](https://doi.org/10.3103/S1062873823702817)
- Aloisio, R., & Berezhinsky, V. 2005, *The Astrophysical Journal*, 625, 249, doi: [10.1086/429615](https://doi.org/10.1086/429615)
- Alvarez-Muñiz, J., Filipčić, A., Lundquist, J. P., et al. 2025, in *UHECR 2024, The 7th International Symposium on Ultra-High-Energy Cosmic Rays*, doi: [10.22323/1.484.0025](https://doi.org/10.22323/1.484.0025)
- Álvarez-Muñiz, J., Alves Batista, R., Balagopal V, A., et al. 2020, *Science China Physics, Mechanics & Astronomy*, 63, 219501, doi: [10.1007/s11433-018-9385-7](https://doi.org/10.1007/s11433-018-9385-7)
- Alves Batista, R., Becker Tjus, J., Dörner, J., et al. 2022, *Journal of Cosmology and Astroparticle Physics*, 2022, 035, doi: [10.1088/1475-7516/2022/09/035](https://doi.org/10.1088/1475-7516/2022/09/035)
- Baldini, P., Buchner, J., Erkenov, A., et al. 2025, arXiv preprint arXiv:2502.08484, doi: [10.48550/arXiv.2502.08484](https://doi.org/10.48550/arXiv.2502.08484)
- Batista, R. A., De Almeida, R. M., Lago, B., & Kotera, K. 2019, *Journal of Cosmology and Astroparticle Physics*, 2019, 002, doi: [10.1088/1475-7516/2019/01/002](https://doi.org/10.1088/1475-7516/2019/01/002)
- Berezhinsky, V., Gazizov, A., & Kalashev, O. 2016, *Astroparticle Physics*, 84, 52, doi: [10.1016/j.astropartphys.2016.08.007](https://doi.org/10.1016/j.astropartphys.2016.08.007)
- Bergman, D. 2021, *PoS, ICRC2021*, 338, doi: [10.22323/1.395.0338](https://doi.org/10.22323/1.395.0338)
- Bister, T., & Farrar, G. R. 2024, *The Astrophysical Journal*, 966, 71, doi: [10.3847/1538-4357/ad2f3f](https://doi.org/10.3847/1538-4357/ad2f3f)
- Borah, D., Das, N., Okada, N., & Sarmah, P. 2025, *Physical Review D*, 111, 123022, doi: [10.1103/shsw-mct6](https://doi.org/10.1103/shsw-mct6)
- Castellina, A. 2019, in *EPJ Web of Conferences*, Vol. 210, EDP Sciences, 06002, doi: [10.1051/epjconf/201921006002](https://doi.org/10.1051/epjconf/201921006002)
- Cermenati, A., Ambrosone, A., Aloisio, R., Boncioli, D., & Evoli, C. 2025, arXiv preprint arXiv:2507.11993, doi: [10.48550/arXiv.2507.11993](https://doi.org/10.48550/arXiv.2507.11993)
- Chen, M., Collaboration, H., et al. 2026, *Nuclear Instruments and Methods in Physics Research Section A: Accelerators, Spectrometers, Detectors and Associated Equipment*, 171374, doi: [10.1016/j.nima.2026.171374](https://doi.org/10.1016/j.nima.2026.171374)
- Comisso, L., Farrar, G. R., & Muzio, M. S. 2024, *Astrophys. J. Lett.*, 977, L18, doi: [10.3847/2041-8213/ad955f](https://doi.org/10.3847/2041-8213/ad955f)
- Das, S., Zhang, B., Razzaque, S., & Xu, S. 2025, *The Astrophysical Journal*, 991, 96, doi: [10.3847/1538-4357/adf8de](https://doi.org/10.3847/1538-4357/adf8de)
- de Clairfontaine, G. F., Perucho, M., & Martí, J. 2025, *Monthly Notices of the Royal Astronomical Society*, staf1929, doi: [10.1093/mnras/staf1929](https://doi.org/10.1093/mnras/staf1929)
- Ehlert, D., Oikonomou, F., & Unger, M. 2023, *Physical Review D*, 107, 103045, doi: [10.1103/PhysRevD.107.103045](https://doi.org/10.1103/PhysRevD.107.103045)
- Ehlert, D., van Vliet, A., Oikonomou, F., & Winter, W. 2024, *Journal of Cosmology and Astroparticle Physics*, 2024, 022, doi: [10.1088/1475-7516/2024/02/022](https://doi.org/10.1088/1475-7516/2024/02/022)
- Feldman, G. J., & Cousins, R. D. 1998, *Physical review D*, 57, 3873, doi: [10.1103/PhysRevD.57.3873](https://doi.org/10.1103/PhysRevD.57.3873)
- Gilmore, R. C., Somerville, R. S., Primack, J. R., & Domínguez, A. 2012, *Monthly Notices of the Royal Astronomical Society*, 422, 3189, doi: [10.1111/j.1365-2966.2012.20841.x](https://doi.org/10.1111/j.1365-2966.2012.20841.x)
- Globus, N., Allard, D., Parizot, E., & Piran, T. 2017, *The Astrophysical journal letters*, 839, L22, doi: [10.3847/2041-8213/aa6af0](https://doi.org/10.3847/2041-8213/aa6af0)
- González, J. M., Mollerach, S., & Roulet, E. 2021, *Phys. Rev. D*, 104, 063005, doi: [10.1103/PhysRevD.104.063005](https://doi.org/10.1103/PhysRevD.104.063005)
- Greisen, K. 1966, *Physical Review Letters*, 16, 748, doi: [10.1103/PhysRevLett.16.748](https://doi.org/10.1103/PhysRevLett.16.748)
- Halim, A. A., Abreu, P., Aglietta, M., et al. 2023, *Journal of Cosmology and Astroparticle Physics*, 2023, 024, doi: [10.1088/1475-7516/2023/05/024](https://doi.org/10.1088/1475-7516/2023/05/024)
- Hasinger, G., Miyaji, T., & Schmidt, M. 2005, *Astronomy & Astrophysics*, 441, 417, doi: [10.1051/0004-6361:20042134](https://doi.org/10.1051/0004-6361:20042134)
- Heinze, J., Boncioli, D., Bustamante, M., & Winter, W. 2016, *The Astrophysical Journal*, 825, 122, doi: [10.3847/0004-637X/825/2/122](https://doi.org/10.3847/0004-637X/825/2/122)
- Heinze, J., Fedynitch, A., Boncioli, D., & Winter, W. 2019, *The Astrophysical Journal*, 873, 88, doi: [10.3847/1538-4357/ab05ce](https://doi.org/10.3847/1538-4357/ab05ce)
- Hopkins, A. M. 2004, *The Astrophysical Journal*, 615, 209, doi: [10.1086/424032](https://doi.org/10.1086/424032)
- Hopkins, A. M., & Beacom, J. F. 2006, *The Astrophysical Journal*, 651, 142, doi: [10.1086/506610](https://doi.org/10.1086/506610)
- Horiuchi, S., Murase, K., Ioka, K., & Meszaros, P. 2012, *The Astrophysical Journal*, 753, 69, doi: [10.1088/0004-637X/753/1/69](https://doi.org/10.1088/0004-637X/753/1/69)
- Kalashev, O. E., Kuzmin, V. A., Semikoz, D. V., & Sigl, G. 2002, *Physical Review D*, 66, 063004, doi: [10.1103/PhysRevD.66.063004](https://doi.org/10.1103/PhysRevD.66.063004)
- Kochanek, C. 2016, *Monthly Notices of the Royal Astronomical Society*, 461, 371, doi: [10.1093/mnras/stw1290](https://doi.org/10.1093/mnras/stw1290)
- Kohri, K., Paul, P. K., & Sahu, N. 2025, *Physical Review D*, 112, L031703, doi: [10.1103/vvqq-1z2t](https://doi.org/10.1103/vvqq-1z2t)
- Koning, A. J., Hilaire, S., & Duijvestijn, M. C. 2007, in *International Conference on Nuclear Data for Science and Technology*, EDP Sciences, 211–214, doi: [10.1051/ndata:07767](https://doi.org/10.1051/ndata:07767)
- Kuznetsov, M. Y., Petrov, N. A., & Savchenko, Y. S. 2025a, arXiv preprint arXiv:2509.09590, doi: [10.48550/arXiv.2509.09590](https://doi.org/10.48550/arXiv.2509.09590)

- Kuznetsov, M. Y., Petrov, N. A., & Savchenko, Y. S. 2025b, arXiv preprint arXiv:2509.09590, doi: [10.48550/arXiv.2509.09590](https://doi.org/10.48550/arXiv.2509.09590)
- Lien, A., Sakamoto, T., Gehrels, N., et al. 2014, *The Astrophysical Journal*, 783, 24, doi: [10.1088/0004-637X/783/1/24](https://doi.org/10.1088/0004-637X/783/1/24)
- Lisanti, M., Mishra-Sharma, S., Necib, L., & Safdi, B. R. 2016, *The Astrophysical Journal*, 832, 117, doi: [10.3847/0004-637X/832/2/117](https://doi.org/10.3847/0004-637X/832/2/117)
- Madau, P., & Dickinson, M. 2014, *Annual Review of Astronomy and Astrophysics*, 52, 415, doi: [10.1146/annurev-astro-081811-125615](https://doi.org/10.1146/annurev-astro-081811-125615)
- Malecki, P. 2024, *Universe*, 10, 53, doi: [10.3390/universe10020053](https://doi.org/10.3390/universe10020053)
- Mayotte, E., Halim, A. A., Abreu, P., et al. 2024, in 38th International Cosmic Ray Conference (ICRC2023)-Cosmic-Ray Physics (Indirect, CRI), Sissa Medialab, 365, doi: [10.22323/1.444.0365](https://doi.org/10.22323/1.444.0365)
- Mollerach, S., & Roulet, E. 2020, *Physical Review D*, 101, 103024, doi: [10.1103/PhysRevD.101.103024](https://doi.org/10.1103/PhysRevD.101.103024)
- Muzio, M. S., Unger, M., & Farrar, G. R. 2019, *Physical Review D*, 100, 103008, doi: [10.1103/PhysRevD.100.103008](https://doi.org/10.1103/PhysRevD.100.103008)
- Muzio, M. S., Unger, M., & Wissel, S. 2023, *Physical Review D*, 107, 103030, doi: [10.1103/PhysRevD.107.103030](https://doi.org/10.1103/PhysRevD.107.103030)
- Muzio, M. S., Yuan, T., & Lu, L. 2025, arXiv preprint arXiv:2502.06944, doi: [10.48550/arXiv.2502.06944](https://doi.org/10.48550/arXiv.2502.06944)
- Neronov, A., Oikonomou, F., & Semikoz, D. 2025, arXiv preprint arXiv:2502.12986, doi: [10.48550/arXiv.2502.12986](https://doi.org/10.48550/arXiv.2502.12986)
- Nozzoli, F. 2025, *Astroparticle Physics*, 103201, doi: [10.1016/j.astropartphys.2025.103201](https://doi.org/10.1016/j.astropartphys.2025.103201)
- Ostapchenko, S., Garzelli, M. V., & Sigl, G. 2023, *Physical Review D*, 107, 023014, doi: [10.1103/PhysRevD.107.023014](https://doi.org/10.1103/PhysRevD.107.023014)
- Peters, B. 1961, *Il Nuovo Cimento (1955-1965)*, 22, 800, doi: [10.1007/BF02783106](https://doi.org/10.1007/BF02783106)
- Petrosian, V., Kitanidis, E., & Kocevski, D. 2015, *The Astrophysical Journal*, 806, 44, doi: [10.1088/0004-637X/806/1/44](https://doi.org/10.1088/0004-637X/806/1/44)
- Petrucci, C., Halim, A. A., Abreu, P., et al. 2024, in 38th International Cosmic Ray Conference (ICRC2023)-Cosmic-Ray Physics (Indirect, CRI), 1520, doi: [10.22323/1.444.1520](https://doi.org/10.22323/1.444.1520)
- Rodrigues, X., Heinze, J., Palladino, A., Van Vliet, A., & Winter, W. 2021, *Physical review letters*, 126, 191101, doi: [10.1103/PhysRevLett.126.191101](https://doi.org/10.1103/PhysRevLett.126.191101)
- Smolčić, V., Zamorani, G., Schinnerer, E., et al. 2009, *The Astrophysical Journal*, 696, 24, doi: [10.1088/0004-637X/696/1/24](https://doi.org/10.1088/0004-637X/696/1/24)
- Stanev, T., Engel, R., Mücke, A., Protheroe, R. J., & Rachen, J. P. 2000, *Physical Review D*, 62, 093005, doi: [10.1103/PhysRevD.62.093005](https://doi.org/10.1103/PhysRevD.62.093005)
- Takami, H., Murase, K., Nagasaki, S., & Sato, K. 2009, *Astroparticle Physics*, 31, 201, doi: [10.1016/j.astropartphys.2009.01.006](https://doi.org/10.1016/j.astropartphys.2009.01.006)
- Taylor, A. M., Ahlers, M., & Hooper, D. 2015, *Physical Review D*, 92, 063011, doi: [10.1103/PhysRevD.92.063011](https://doi.org/10.1103/PhysRevD.92.063011)
- Thoudam, S., Rachen, J., Van Vliet, A., et al. 2016, *Astronomy & Astrophysics*, 595, A33, doi: [10.1051/0004-6361/201628894](https://doi.org/10.1051/0004-6361/201628894)
- Ueda, Y., Akiyama, M., Hasinger, G., Miyaji, T., & Watson, M. G. 2014, *The Astrophysical Journal*, 786, 104, doi: [10.1088/0004-637X/786/2/104](https://doi.org/10.1088/0004-637X/786/2/104)
- Ueda, Y., Akiyama, M., Ohta, K., & Miyaji, T. 2003, *The Astrophysical Journal*, 598, 886, doi: [10.1086/378940](https://doi.org/10.1086/378940)
- van Vliet, A., Batista, R. A., & Hörandel, J. R. 2019, *Physical Review D*, 100, 021302, doi: [10.1103/PhysRevD.100.021302](https://doi.org/10.1103/PhysRevD.100.021302)
- Wanderman, D., & Piran, T. 2010, *Monthly Notices of the Royal Astronomical Society*, 406, 1944, doi: [10.1111/j.1365-2966.2010.16787.x](https://doi.org/10.1111/j.1365-2966.2010.16787.x)
- Wittkowski, D., Albuquerque, I. F. d. M., Catalani, F., et al. 2017, *Proceedings of Science*, 301, 563, doi: [10.22323/1.301.0563](https://doi.org/10.22323/1.301.0563)
- Ye, Z., Hu, F., Tian, W., et al. 2023, *Nature Astronomy*, 7, 1497, doi: [10.1038/s41550-023-02087-6](https://doi.org/10.1038/s41550-023-02087-6)
- Yüksel, H., Kistler, M. D., Beacom, J. F., & Hopkins, A. M. 2008, *The Astrophysical Journal Letters*, 683, L5, doi: [10.1086/591449](https://doi.org/10.1086/591449)
- Zatsepin, G. T., & Kuz'min, V. A. 1966, *Soviet Journal of Experimental and Theoretical Physics Letters*, 4, 78
- Zhang, H., Cui, Y., Huang, Y., et al. 2025, *Astroparticle Physics*, 171, 103123, doi: [10.1016/j.astropartphys.2025.103123](https://doi.org/10.1016/j.astropartphys.2025.103123)